

A slowly rotating hollow sphere in a magnetic field: First steps to de-spin a space object

Robert C. Youngquist, Mark A. Nurge, and Stanley O. StarrFrederick A. LeveMason Peck

Citation: [Am. J. Phys.](#) **84**, (2016); doi: 10.1119/1.4936633

View online: <http://dx.doi.org/10.1119/1.4936633>

View Table of Contents: <http://aapt.scitation.org/toc/ajp/84/3>

Published by the [American Association of Physics Teachers](#)

A slowly rotating hollow sphere in a magnetic field: First steps to de-spin a space object

Robert C. Youngquist,^{a)} Mark A. Nurge,^{b)} and Stanley O. Starr^{c)}

National Aeronautics and Space Administration, Mail Code: UBR3, Kennedy Space Center, Florida 32899

Frederick A. Leve^{d)}

Air Force Research Laboratory, Kirtland Air Force Base, New Mexico 87117

Mason Peck^{e)}

208 Upson Hall, Sibley School of Mechanical and Aerospace Engineering, Cornell University, 124 Hoy Road, Ithaca, New York 14853

(Received 3 June 2015; accepted 12 November 2015)

Modeling the interaction of a slowly rotating hollow conducting sphere in a magnetic field provided an understanding of the dynamics of orbiting space objects moving through the Earth's magnetic field. This analysis, performed in the late 1950s and limited to uniform magnetic fields, was innovative and acknowledged the pioneers who first observed rotary magnetism, in particular, the seminal work of Hertz in 1880. Now, there is interest in using a magnetic field produced by one space object to stop the spin of a second object so that docking can occur. In this paper, we consider, yet again, the interaction of a rotating hollow sphere in a magnetic field. We show that the predicted results can be tested experimentally, making this an interesting advanced student project. This analysis also sheds light on a rich set of previously unaddressed behaviors involving eddy currents. © 2016 American Association of Physics Teachers.

[<http://dx.doi.org/10.1119/1.4936633>]

I. INTRODUCTION

In the 1950s, with the advent of the space U.S. program, there was a surge of interest in modeling the interaction of spinning space objects with the Earth's magnetic field.^{1–5} This work assumed a uniform magnetic field and modeled the space objects as either hollow spheres or cylinders. The most detailed and complete analysis of a hollow conducting sphere slowly rotating in a uniform magnetic field was carried out by Vinti.¹ In this work, he produced an expression for the drag torque felt by the space object that causes it to slowly de-spin, predicting decay times on the order of months. This result was substantiated by space object observation and used to provide estimates of the magnitude of the Earth's magnetic field at various altitudes.^{6–9}

These space program scientists acknowledged their debt to the earlier work of the 1800s and its continued development through the 1930s. Arago first noticed induced magnetism in rotating objects in 1824.¹⁰ Faraday helped to explain this when he discovered in 1831 that conductors moving through a magnetic field generate a voltage, but analyzing the specific problem of a hollow sphere rotating in a magnetic field required Maxwell's equations (1861) and was solved in 1880 by the then 23-year old Hertz.¹¹ However, this was four years before Heaviside introduced the modern form of Maxwell's equations with vector notation, so Hertz's work can be difficult for a modern reader to follow. Even so, Hertz's work is more general than that of the early space program researchers in that he carried out his analysis for a hollow sphere rotating at any speed, located in a non-uniform, constant magnetic field.

This more general aspect of Hertz's work makes it applicable to an area of growing interest within the space community, namely, de-spinning rotating orbiting satellites or space debris. There are a large number of defunct satellites in orbit that could be made operational again with refueling, or space debris to be removed from orbit in a non-destructive manner.

However, mechanical attachment is difficult if the space object (defunct satellite or a piece of space debris) is spinning with respect to a servicing spacecraft. Bennett *et al.*¹² give more background on this problem while considering the possibility of using electrostatics as a means of de-spinning a space object. Our goal is to consider the alternative approach of using the magnetic field from a spacecraft to de-spin a tumbling space object sufficiently so that mechanical docking can be achieved. This approach has been discussed in two recent publications,^{9,13} but both of these only consider a uniform magnetic field.

There are two goals of this paper. The first is to determine the feasibility of de-spinning a rotating space object using the interaction with a constant, non-uniform magnetic field, and the second is to understand the physics so that tests can be performed to verify the theory. With this in mind we chose (akin to the development from the early space program) to model the space object as a hollow sphere, in this case a thin walled spherical shell. Since most space objects have a thin conductive outer shell, this is a reasonable choice physically and mathematically as it allows the problem to be solved analytically, which has pedagogical value. We recognize that angular momentum is conserved and that de-spinning one space object will cause the servicing spacecraft to move oppositely, but we assume that thrusters can be employed to prevent this, allowing a fixed orientation to be maintained between the spacecraft and the space object during the de-spinning process.

The interaction of a space object with Earth's magnetic field causes it to de-spin over long time periods.^{6–9} However, other effects such as radiation pressure can also generate a small accelerating torque.¹⁴ So most space objects rotate slowly, typically a few revolutions per minute.⁶ This is still too fast to allow docking but allows a significant simplification to the analysis. A rapidly rotating sphere may itself generate a significant magnetic field, which will affect the sphere's eddy currents. The change in the eddy currents then

changes the magnetic field, resulting in an infinite feedback process. Hertz handles the analysis in exactly this manner, expressing every term and summing the results.¹¹ However, due to the slow rotation rate of space objects, we (like the early space program analysts) can ignore this feedback process. Even so, we will verify in our analysis that the magnitude of the sphere's induced magnetic field is small compared to the applied magnetic field.

II. GENERAL COMMENTS ON THE PROBLEM

The interaction of a constant magnetic field with a moving extended conductor is an important area of study with applications to linear induction motors, eddy current braking, and levitation. However, this topic is inadequately handled in most modern textbooks on electromagnetism. Some texts, such as Jackson¹⁵ and Schwinger,¹⁶ ignore this topic, while others qualitatively discuss eddy current generation or present the simple case of the Faraday Disk (Lorrain and Corson¹⁷ and Griffiths¹⁸). In essence, the material presented in the textbooks we examined is inadequate to solve the problem of a rotating hollow sphere in a uniform magnetic field. Yet this problem has historical relevance being solved by Hertz, has application to the dynamics of satellites and the early measurements of Earth's magnetic field, and is within the grasp of an advanced undergraduate.

When an extended, isolated conductor moves through a constant magnetic field, forces are exerted on the electrons in the conductor. It is often assumed that eddy currents result, but this is not always the case, as will be shown below. In the general case, the electrons will redistribute themselves, generating a non-uniform charge density that will create electric fields within the conductor. So the first step in analyzing this problem will be to find the induced charge density, and then to find the potential and the electric field that correspond to it. Then, the electric and magnetic field forces are combined and any net forces create current flow within the conductor. The details of this process will be presented in Secs. III–VI. However, this is not meant to be a general introduction to this area but instead is an exposition on a problem beyond the material in modern textbooks.

Sections III and IV will model two cases of the slowly rotating hollow sphere, starting with the simplest case of the sphere spinning about an axis aligned with an applied uniform magnetic field, then moving to a perpendicular rotation axis, and in Secs. V and VI repeating these two orientations with non-uniform magnetic fields that are cylindrically symmetric about the z -axis. The sphere will have a radius given by a and a wall thickness given by $h \ll a$. The conductivity of the sphere is given by σ , and the material density of the sphere is given by ρ_m . The total mass of the sphere is then $m = 4\pi a^2 h \rho_m$ and the sphere's moment of inertia is, $I = (2/3)ma^2 = (8/3)\pi a^4 h \rho_m$. In all cases, the sphere will be rotating at angular frequency ω about the z -axis, i.e., $\vec{\omega} = \omega \hat{z}$. We are only interested in steady state results, as transients in conductors die out rapidly, so all the fields, potentials, currents, and charge densities are time independent as seen from the laboratory frame. Some authors chose to work in the frame of the sphere and adopt a time varying magnetic field,¹⁹ but we believe this adds unnecessary complications, so the analysis below is performed in the laboratory frame of reference. Finally, it is assumed that the sphere has no net charge.

III. UNIFORM FIELD PARALLEL TO ROTATION AXIS

This case was developed by Hertz¹¹ and Vinti,¹ while Lorrain²⁰ recently analyzed the spinning solid sphere. We repeat the derivation in order to develop notation and concepts before addressing the more complicated cases. The reader may find it useful to consult the helpful relationships between spherical and Cartesian coordinate systems that can be found in many textbooks.¹⁸ Figure 1 shows the basic geometry, including the Cartesian and spherical coordinate systems, with the z -axis aligned with both the applied field $\vec{B} = B \hat{z}$ and the rotation vector $\vec{\omega}$.

Since the sphere is rotating, material is moving through the applied magnetic field, and from the Lorentz force law this generates forces on the charges proportional to $\vec{v} \times \vec{B}$, where \vec{v} is the velocity of the charges. Because the sphere is neutral, the forces on the positive and negative charges approximately cancel. However, since the sphere is conductive the electrons can move while the protons remain fixed, and this can result in charge redistribution and possible currents. The goal of the analysis is to determine what (if any) forces and torques are felt by the sphere as a result of these charge redistributions and currents.

To begin, we define a vector of length a that points to each location on the surface of the hollow sphere as

$$\vec{a} = \{a \sin \theta \cos \phi, a \sin \theta \sin \phi, a \cos \theta\}. \quad (1)$$

Using this, the velocity of any point on the sphere is given by

$$\begin{aligned} \vec{v} &= \vec{\omega} \times \vec{a} = -\omega a \sin \theta \sin \phi \hat{x} + \omega a \sin \theta \cos \phi \hat{y} \\ &= \omega a \sin \theta \hat{\phi}. \end{aligned} \quad (2)$$

This expression assumes that the hollow sphere's wall thickness h is small compared to the sphere radius a , an assumption that will be used repeatedly in the following analysis. We need to find the charge distributions and currents caused by the magnetic field. To do this, express the Lorentz Force Law as a generalized Ohm's law

$$\vec{J} = \sigma \vec{E} + \sigma \vec{v} \times \vec{B}, \quad (3)$$

where \vec{J} is the current density and \vec{E} is the electric field caused by the charge distribution. The conservation of

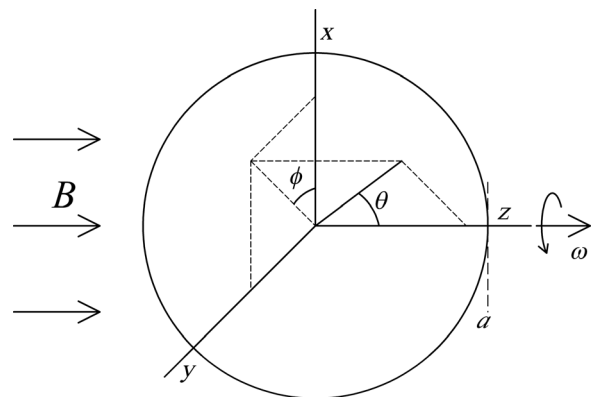


Fig. 1. The basic geometry and coordinate systems used to model a rotating hollow sphere when the rotation axis is aligned with an applied uniform magnetic field.

charge expression is $\vec{\nabla} \cdot \vec{J} = -\partial\rho/\partial t$, but since we are only concerned with steady-state situation, where the charge distribution is constant, we have

$$\vec{\nabla} \cdot \vec{J} = 0 \quad (4)$$

for all currents in all cases being considered.

Taking the divergence of Eq. (3) and using Eq. (4) yields

$$\vec{\nabla} \cdot \vec{E} = -\vec{\nabla} \cdot (\vec{v} \times \vec{B}), \quad (5)$$

and we recall from Gauss's law that the divergence of the electric field is the charge distribution. However, before making this association we need to consider the geometry of the problem. The charge distributions and currents are restricted in that charges cannot leave the shell and this limitation must be captured by the mathematics. We do this by making the assumption that steady-state currents cannot flow radially in a thin shell and can thus only have tangential components. Figure 2 shows this assumption graphically. The magnetic force (per unit charge) has a radial component, which, because there is no radial current, must be equal and opposite to the radial electric field. But the radial electric field is the result of charges distributed between the inner and outer surface of the sphere. Now, because the sphere is a thin shell, these charges will be close to each other and will therefore approximately cancel, yielding no net forces or torques on the sphere. So, in all of the analyses below the radial component of the magnetic force will be ignored, and only the tangential components will be considered (tangential vector components will be shown with a "t" subscript). Referring to Fig. 2 again, we see that the tangential component of the magnetic force is composed of some combination of the (tangential) electric field and the current.

Now, using the velocity from Eq. (2), we can write

$$\begin{aligned} \vec{v} \times \vec{B} &= \omega a B \sin \theta (\cos \phi \hat{x} + \sin \phi \hat{y}) \\ &= \omega a B \sin \theta (\sin \theta \hat{r} + \cos \theta \hat{\theta}). \end{aligned} \quad (6)$$

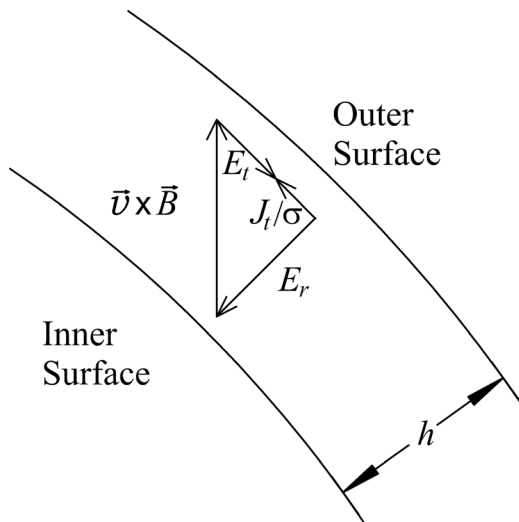


Fig. 2. A small section of the rotating sphere shows the direction of the force density on the charges in the moving conductor and the compensating electric field components and current.

We can define a tangential charge density ρ_t by taking the divergence of the tangential portion of this magnetic force and using Eq. (4) and Gauss's law to obtain

$$\begin{aligned} \rho_t &= \epsilon_0 \vec{\nabla} \cdot \vec{E}_t = -\epsilon_0 \vec{\nabla} \cdot (\vec{v} \times \vec{B})_t \\ &= -\epsilon_0 \vec{\nabla} \cdot (\omega a B \sin \theta \cos \theta \hat{\theta}) \\ &= -\epsilon_0 \omega B (2 \cos^2 \theta - \sin^2 \theta) \\ &= -2\epsilon_0 \omega B P_2^0(\cos \theta), \end{aligned} \quad (7)$$

where P_2^0 is a Legendre polynomial (see Appendix B). This charge distribution is shown in Fig. 3 where positive charge (red) has been pushed to the fastest-moving equatorial portion of the sphere, leaving negative charge (blue) at the poles.

So we have the charge distribution, but we don't know the currents. To solve for the current density, we need to find the tangential electric field \vec{E}_t and then substitute this into Ohm's Law [Eq. (3)]. To find the electric field, we can solve Poisson's equation for the potential Φ_t arising from the charge distribution

$$-\vec{\nabla} \cdot \vec{E}_t = \vec{\nabla}^2 \Phi_t = -\rho_t / \epsilon_0 = 2\omega B P_2^0(\cos \theta). \quad (8)$$

Using Eq. (A3) from Appendix A, the corresponding potential is

$$\Phi_t(\theta) = -\frac{\omega a^2 B}{3} P_2^0(\cos \theta) = \frac{\omega a^2 B}{6} (3 \cos^2 \theta - 1). \quad (9)$$

Thus, the tangential electric field becomes

$$\vec{E}_t = -\omega a B \sin \theta \cos \theta \hat{\theta}, \quad (10)$$

which is equal and opposite to the tangential magnetic force, $(\vec{v} \times \vec{B})_t$, showing that there is no current density ($\vec{J} = 0$) in this case. This makes intuitive sense, as the charges have been pushed to a cylindrically symmetric configuration where they see a constant force as the sphere rotates, so a

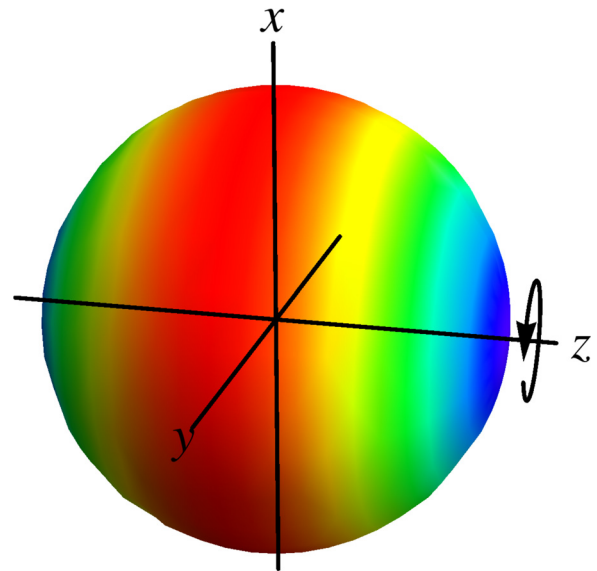


Fig. 3. (Color online) The charge distribution on a rotating spherical shell in a uniform magnetic field along the z-axis. The positive charge (red) lies at the equator near the $z=0$ crossing of the x-y plane. The negative charge (blue) lies at the poles at either end of the z-axis, near where $x=0$ and $y=0$.

steady state can be achieved without currents. So in this first case there are no currents and thus no forces or torques on the sphere, in agreement with the results in the literature.

Before concluding this section, one might argue that the rotation of the sphere carries a charge distribution with it and creates a net current about the z -axis. This is indeed correct. When charge is carried by a moving entity it generates an advection current²¹ (as opposed to an Ohmic current), where the electrons move relative to the conductor. However, due to the very small charge density—note the factor of $\epsilon_0 = 8.85 \times 10^{-12}$ F/m in Eq. (7)—and the sphere's slow rotation velocity, the advection current here is very small, on the order of nanoAmperes, and can thus be ignored here and in Secs. IV–VIII.

IV. UNIFORM FIELD PERPENDICULAR TO ROTATION AXIS

This case best describes the interaction of a space object with the Earth's magnetic field and was studied extensively in the late 1950s. The coordinate system is shown in Fig. 4 with the sphere spinning about the x -axis and the applied field aligned with the z -axis, $\vec{B} = B\hat{z}$. The rotation vector is given by $\vec{\omega} = \omega\hat{x}$ so the velocity vector is

$$\vec{v} = \vec{\omega} \times \vec{a} = -\omega a \cos \theta \hat{y} + \omega a \sin \theta \sin \phi \hat{z}. \quad (11)$$

The magnetic force generated by the motion of the shell is now given by

$$\begin{aligned} \vec{v} \times \vec{B} &= -\omega a \cos \theta B \hat{x} \\ &= -\omega a \sin \theta \cos \theta \cos \phi B \hat{r} \\ &\quad - \omega a \cos^2 \theta \cos \phi B \hat{\theta} + \omega a \cos \theta \sin \phi B \hat{\phi} \end{aligned} \quad (12)$$

and is directed along the x -axis. As before, we can find the resulting tangential charge density by taking the divergence of the tangential portion of the magnetic force (see Appendix B), giving

$$\begin{aligned} \rho_t &= \epsilon_0 \vec{\nabla} \cdot \vec{E}_t = -\epsilon_0 \vec{\nabla} \cdot (\vec{v} \times \vec{B})_t \\ &= -\epsilon_0 \vec{\nabla} \cdot (-\omega a \cos^2 \theta \cos \phi B \hat{\theta} + \omega a \cos \theta \sin \phi B \hat{\phi}) \\ &= -3\epsilon_0 \omega B \cos \theta \sin \theta \cos \phi \\ &= \epsilon_0 \omega B P_2^1(\cos \theta) \cos \phi, \end{aligned} \quad (13)$$

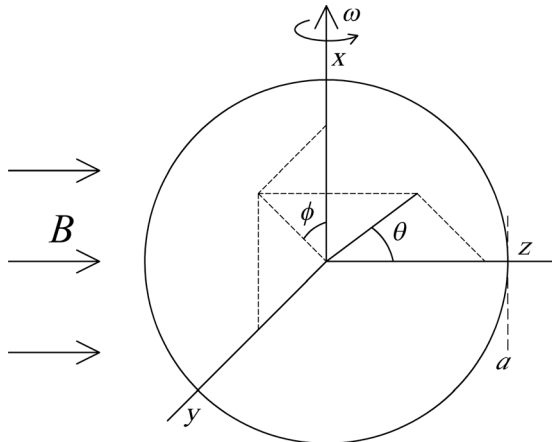


Fig. 4. The basic geometry and coordinate systems used to model a rotating hollow sphere when the rotation axis is perpendicular to an applied uniform magnetic field.

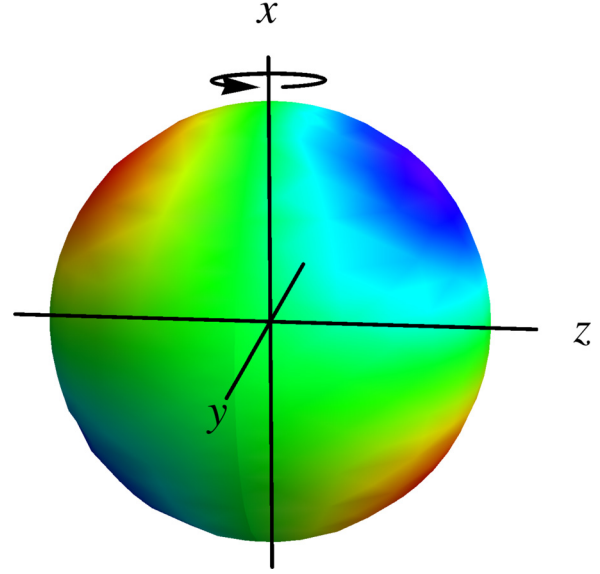


Fig. 5. (Color online) The charge distribution on a spherical shell spinning perpendicular to a uniform magnetic field along the z -axis. The positive charge (red) congregates near $y=0$ where x and z have opposite signs while the negative charge (blue) congregates near $y=0$ where x and z have the same signs.

and yielding the charge distribution shown in Fig. 5.

We want to find the electric field created by this tangential charge density. So, starting with Poisson's equation

$$-\vec{\nabla} \cdot \vec{E}_t = \vec{\nabla}^2 \Phi_t = -\rho_t / \epsilon_0 = -\omega B P_2^1(\cos \theta) \cos \phi. \quad (14)$$

Eq. (A3) can be applied to find the corresponding potential

$$\begin{aligned} \Phi_t(\theta, \phi) &= \frac{\omega a^2 B}{6} P_2^1(\cos \theta) \cos \phi \\ &= -\frac{\omega a^2 B}{2} \cos \theta \sin \theta \cos \phi. \end{aligned} \quad (15)$$

The tangential electric field within the shell then becomes

$$\vec{E}_t = \frac{\omega a B}{2} (1 - 2 \sin^2 \theta) \cos \phi \hat{\theta} - \frac{\omega a B}{2} \cos \theta \sin \phi \hat{\phi}. \quad (16)$$

Inserting this expression into Eq. (3), along with the tangential magnetic force, yields the current density within the rotating hollow sphere

$$\begin{aligned} \vec{J} &= -\frac{\sigma \omega a B}{2} \cos \phi \hat{\theta} + \frac{\sigma \omega a B}{2} \cos \theta \sin \phi \hat{\phi} \\ &= \frac{\sigma \omega a B}{2} (-\cos \theta \hat{x} + \sin \theta \cos \phi \hat{z}). \end{aligned} \quad (17)$$

Unlike the previous case where the electric and magnetic Lorentz forces cancel each other, they now give rise to a circular current flow about the y -axis, as shown in Fig. 6. Clearly, the condition that the divergence of the current density be zero has been satisfied.

We can now calculate the net force and torque on the sphere that results from this current density interacting with the applied field. First, the net force on the sphere is found to be zero by integrating the cross product of the current density and the applied magnetic field through the volume of the hollow sphere

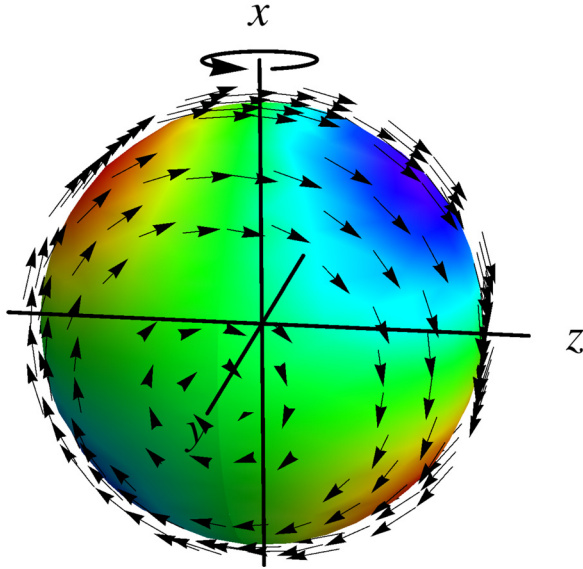


Fig. 6. (Color online) The current density on a spherical shell forms circles about the y-axis. The shell is spinning about the x-axis in a uniform magnetic field along the z-direction. The underlying charge density is as in Fig. 5.

$$\begin{aligned}\vec{F} &= \int_V \vec{J} \times \vec{B} dV \\ &= \frac{\sigma\omega a B^2 h}{2} \int_0^{2\pi} \int_0^\pi a^2 \cos\theta \sin\theta \hat{y} d\theta d\phi = 0.\end{aligned}\quad (18)$$

The net torque, however, is not zero and is the reason for the interest in this work during the early space program. Using Eq. (17), the net torque $\vec{\tau}$ is given by

$$\begin{aligned}\vec{\tau} &= \int_V \vec{a} \times (\vec{J} \times \vec{B}) dV \\ &= \frac{\sigma\omega a B^2}{2} \int_V \vec{a} \times (\cos\theta \hat{y}) dV \\ &= -\frac{\sigma\omega B^2 a^2}{2} \int_V \cos^2\theta \hat{x} dV + \frac{\sigma\omega B^2 a^2}{2} \\ &\quad \times \int_V \sin\theta \cos\theta \cos\phi \hat{z} dV \\ &= -\frac{\sigma\omega B^2 a^4 h}{2} \int_0^{2\pi} \int_0^\pi \cos^2\theta \sin\theta \hat{x} d\theta d\phi \\ &= -\frac{2\pi\sigma\omega B^2 a^4 h}{3} \hat{x},\end{aligned}\quad (19)$$

agreeing with the results in the literature.²

Equation (19) can be put into a more useful form by recalling that torque is equal to the moment of inertia times the rate of change in angular velocity. For the spinning shell, this becomes

$$\vec{\tau} = I \frac{\partial\omega}{\partial t} \hat{x} = \frac{8\pi a^4 h \rho_m}{3} \frac{\partial\omega}{\partial t} \hat{x}. \quad (20)$$

Combining this with Eq. (19) yields

$$\frac{4\rho_m}{\sigma B^2} \frac{\partial\omega}{\partial t} = -\omega, \quad (21)$$

which indicates that the spinning shell decelerates exponentially ($\omega \propto e^{-t/\alpha}$) with a time constant

$$\alpha = \frac{4\rho_m}{\sigma B^2}. \quad (22)$$

This surprisingly simple result is independent of the shell radius or thickness and agrees with the literature. It shows that a spinning aluminum shell in orbit, where Earth's magnetic field is about $25 \mu\text{T}$, has a decay time of about a week. If we approach an aluminum space object with a uniform 1-mT field, the decay time will be about 5 min. This bodes well for our application, but generating a uniform magnetic field over an entire space object is difficult. It would be preferable to be able to approach a rotating space object from one side with a coil or magnet that generates a non-uniform magnetic field; this will be the topic of discussion in Secs. V and VI.

However, before moving to the next case, we digress briefly to explain why we are limited to slowly rotating spheres. The current \vec{J} expressed in Eq. (17) generates a uniform magnetic field \vec{B}_{s1} within the hollow sphere¹⁸ given by

$$\vec{B}_{s1} = -\frac{\mu_0 \sigma \omega B a h}{3} \hat{y} \equiv -\beta B \hat{y}. \quad (23)$$

This expression defines a dimensionless parameter β , as the ratio of the (interior) magnetic field amplitude created by the induced current to the applied magnetic field amplitude. As an example, if a space object with a 1-cm-thick aluminum shell ($\sigma = 3.6 \times 10^7 \text{ S/m}$) and a radius of 1 m were spinning at 1/2 Hz, then $\beta \approx 0.47$. In this example, the sphere's induced magnetic field is significant and it will generate additional eddy currents, so we need to consider this process in more detail.

Recall that the original magnetic field is directed along the z-axis and that the rotating sphere generates an internal uniform magnetic field \vec{B}_{s1} pointing in the negative y-direction. This generated field will, through the same process, generate another magnetic field \vec{B}_{s2} , directed in the negative z-direction. This second-order-generated magnetic field is opposed to the original field \vec{B} and partially cancels it, reducing the net field along the z-direction. The amplitudes of the magnetic fields thus satisfy

$$B_{s1} = -\beta(B - B_{s2}) \quad \text{and} \quad B_{s2} = -\beta B_{s1}, \quad (24)$$

which can be solved to obtain

$$B_{s1} = \frac{-\beta B}{1 + \beta^2}, \quad B_{s2} = \frac{\beta^2 B}{1 + \beta^2}, \quad \text{and} \quad B - B_{s2} = \frac{B}{1 + \beta^2}. \quad (25)$$

If β is small, the incoming magnetic field enters the sphere and creates only the first magnetic field \vec{B}_{s1} (i.e., $B_{s2} \approx 0$). However, if β is large then the second magnetic field \vec{B}_{s2} grows to almost cancel the incoming field (i.e., $B_{s2} \approx B$). The small remnant that gets through to the sphere is "amplified" once to create \vec{B}_{s1} and again to create \vec{B}_{s2} . Looking at Eq. (25), one can see that as β becomes significant in size, the magnetic field in the sphere, and the accompanying torque, is reduced by a factor of $1 + \beta^2$, and the decay time in Eq. (22) is increased by this factor squared.

For the present case, where we desire to use a magnetic field to de-spin a space object, we have to be aware that this effect occurs. We thus require that the space objects have a small angular velocity, such that

$$\beta \ll 1 \Rightarrow \omega \ll \frac{3}{\mu_0 \sigma a h}. \quad (26)$$

This condition will ensure that the applied magnetic field enters the rotating sphere and is not (significantly) reduced by a second-order induced field.

V. NON-UNIFORM FIELD PARALLEL TO ROTATION AXIS

What happens if we approach a rotating space object along its rotation axis and expose it to a non-uniform, but constant, magnetic field that is symmetrical about the rotation axis (e.g., generated by a coil or magnet)? Using the same coordinate configuration as shown in Fig. 1, such a magnetic field can be written

$$\vec{B}(r, \theta) = B_r(r, \theta) \hat{r} + B_\theta(r, \theta) \hat{\theta}. \quad (27)$$

The velocity of the hollow sphere is still given by Eq. (2), so after some manipulation it can be shown that

$$\vec{v} \times \vec{B} = -\omega a \sin \theta B_\theta(a, \theta) \hat{r} + \omega a \sin \theta B_r(a, \theta) \hat{\theta}. \quad (28)$$

Our intuition, based on the first case, suggests that this magnetic force should distribute the charge symmetrically around the z -axis and there should be no resulting currents. This is exactly what happens, but by going through the math we will start to develop the tools needed to handle the more complicated non-uniform perpendicular magnetic field case. So we proceed along the same path as in the first case above, with one significant addition in that we choose to decompose the radial portion of the magnetic field into a sum of Legendre polynomials in $\cos \theta$ (as proposed by Hertz¹¹). Mathematically,

$$B_r(a, \theta) = \sum_{n=1}^{\infty} b_n P_n^0(\cos \theta), \quad (29)$$

where

$$b_n = \frac{2n+1}{2} \int_0^\pi B_r(a, \theta) P_n^0(\cos \theta) \sin \theta d\theta. \quad (30)$$

The summation starts at $n=1$ because the $n=0$ term corresponds to a magnetic monopole term. Combining the above relationships and using the properties of Legendre polynomials (see Appendix B), we find that the tangential charge density can be written as

$$\begin{aligned} \rho_t &= \epsilon_0 \vec{\nabla} \cdot \vec{E}_t \\ &= -\epsilon_0 \vec{\nabla} \cdot [\omega a \sin \theta B_r(a, \theta) \hat{\theta}] \\ &= -\epsilon_0 \omega a \sum_{n=1}^{\infty} b_n \vec{\nabla} \cdot [\sin \theta P_n^0(\cos \theta) \hat{\theta}] \\ &= -\epsilon_0 \omega \sum_{n=1}^{\infty} b_n \left[\frac{(2+n)(n+1)}{2n+1} P_{n+1}^0(\cos \theta) \right. \\ &\quad \left. - \frac{(n-1)n}{2n+1} P_{n-1}^0(\cos \theta) \right]. \end{aligned} \quad (31)$$

Now, using Eq. (A3) the potential $\Phi(\theta)$ corresponding to this charge density is found to be

$$\Phi(\theta) = \omega a^2 \sum_{n=1}^{\infty} \frac{b_n}{2n+1} [P_{n+1}^0(\cos \theta) - P_{n-1}^0(\cos \theta)]. \quad (32)$$

Taking the θ derivative, with the help of Eq. (B5), the electric field is then

$$\vec{E}_t = -\omega a \sin \theta \sum_{n=1}^{\infty} b_n P_n^0(\cos \theta) \hat{\theta} = -(\vec{v} \times \vec{B})_t, \quad (33)$$

which generates a force that is equal and opposite to the magnetic force [see Eq. (28)]. The charge distribution generates an electric field that cancels the magnetic force, proving that there are no induced currents in this case. So bringing a static, axially symmetric, non-uniform magnetic field near a rotating space object along its rotation axis produces no forces or torques.

VI. NON-UNIFORM PERPENDICULAR TO ROTATION AXIS

This is the most important case when applied to space object de-spinning but is also the most complicated to analyze. We will use the tools developed in Secs. II–V and add some additional structure in order to achieve the goal of determining the force and torque on the sphere under the influence of a non-uniform magnetic field. We use the same coordinate system as in the other cases with the sphere rotating about the x -axis as shown in Fig. 4.

We can represent the applied magnetic field in the same manner as for the previous case, where Eqs. (27), (29), and (30) are all valid. Meanwhile, the velocity \vec{v} is given by Eq. (11). Combining these, the magnetic force density can be found to be

$$\begin{aligned} \vec{v} \times \vec{B} &= a\omega B_\theta \cos \theta \cos \phi \hat{r} - a\omega B_r \cos \theta \cos \phi \hat{\theta} \\ &\quad + a\omega B_r \sin \phi \hat{\phi}. \end{aligned} \quad (34)$$

We are only interested in the tangential force, which only depends on the radial portion of the magnetic field, so we can find the charge density using the same approach as in Secs. II–V

$$\begin{aligned} \rho_t &= -\epsilon_0 \vec{\nabla} \cdot (\vec{v} \times \vec{B})_t \\ &= \epsilon_0 a\omega \vec{\nabla} \cdot [B_r(a, \theta) \cos \theta \cos \phi \hat{\theta} - B_r(a, \theta) \sin \phi \hat{\phi}] \\ &= -\epsilon_0 \omega \cos \phi \left[2 \sin \theta B_r(a, \theta) - \cos \theta \frac{\partial B_r(a, \theta)}{\partial \theta} \right]. \end{aligned} \quad (35)$$

Now we can decompose the radial portion of the applied magnetic field into a sum of Legendre polynomials as in Eq. (29) to obtain (see Appendix B)

$$\begin{aligned} \rho_t &= \epsilon_0 \omega \cos \phi \sum_{n=1}^{\infty} \frac{b_n}{2n+1} \\ &\quad \times [(n-1)P_{n-1}^1(\cos \theta) + (n+2)P_{n+1}^1(\cos \theta)]. \end{aligned} \quad (36)$$

From this, the potential can be found using Appendix B and Eq. (A3) to be

$$\Phi(\theta, \phi) = \omega a^2 \cos \phi \cos \theta \sum_{n=1}^{\infty} \frac{b_n}{n(n+1)} P_n^1(\cos \theta). \quad (37)$$

Using this potential the electric field can be found, allowing the current density to be calculated [see Eqs. (B9) and (B10)] as

$$\begin{aligned}\vec{J} &= \sigma \vec{E}_t + \sigma(\vec{v} \times \vec{B})_t = \sigma[-\vec{\nabla}\Phi(\theta, \phi) + (\vec{v} \times \vec{B})_t] \\ &= \sum_{n=1}^{\infty} \frac{b_n \sigma a \omega}{2} \left\{ -\cos \phi \left[P_{n-1}^0(\cos \theta) + \frac{P_{n-1}^2(\cos \theta)}{n(1+n)} \right] \hat{\theta} \right. \\ &\quad \left. + \sin \phi \left[P_n^0(\cos \theta) - \frac{P_n^2(\cos \theta)}{n(1+n)} \right] \hat{\phi} \right\}. \quad (38)\end{aligned}$$

The divergence of this current is zero and its curl equals the curl of the tangential portion of the magnet force, indicating that it is the correct solution. Plotting this current expression for different values of n yields vector plots of closed contours on the sphere with increasing numbers of symmetrical loops.

Now that we've found the current, the task is to find the net force and torque on the sphere, and to do this we need to find the force density given by $\vec{J} \times \vec{B}$, which is

$$\begin{aligned}\vec{J} \times \vec{B} &= \sum_{n=1}^{\infty} \frac{b_n \sigma a \omega}{2} \left\{ B_{\theta} \sin \phi \left[-P_n^0(\cos \theta) + \frac{P_n^2(\cos \theta)}{n(1+n)} \right] \hat{r} \right. \\ &\quad + B_r \sin \phi \left[P_n^0(\cos \theta) - \frac{P_n^2(\cos \theta)}{n(1+n)} \right] \hat{\theta} \\ &\quad \left. + B_r \cos \phi \left[P_{n-1}^0(\cos \theta) + \frac{P_{n-1}^2(\cos \theta)}{n(1+n)} \right] \hat{\phi} \right\}. \quad (39)\end{aligned}$$

Converting this expression to Cartesian coordinates and then integrating over the spherical shell [see Eq. (18)] shows that there is no net force in the x - or z -directions, but there is a net force in the y -direction that depends on B_{θ} but not on B_r .

Thus, in order to proceed we expand B_{θ} in terms of the Legendre Polynomials to get

$$B_{\theta}(a, \theta) = \frac{1}{\sin \theta} \sum_{i=0}^{\infty} c_i P_i^0(\cos \theta). \quad (40)$$

Using this expansion in Eq. (39) leads to a complicated expression; however, most of the terms go to zero. Even so, we were not able to obtain a general analytic expression for the transverse force on the sphere and instead used MATHEMATICA to obtain

$$\begin{aligned}\vec{F} &= \frac{a^3 h \sigma \omega \pi}{2} \left[\sum_{n=1}^{\infty} \frac{4(n+1)b_n b_{n+1}}{(2n+1)(2n+3)} \right. \\ &\quad + \sum_{i=0}^{\infty} \sum_{n=1}^{\infty} \frac{2b_{2n+i} c_i}{(2n+i)(2n+i+1)} \\ &\quad \left. - \sum_{n=1}^{\infty} \frac{2nb_n c_n}{(n+1)(2n+1)} \right] \hat{y} \quad (41)\end{aligned}$$

for the lateral force.

Equation (41) is an important, albeit complicated, result. To get a feeling for the order of magnitude of the force, consider the 1-m radius space object example used in Sec. IV. If we assume 1 mT field components for b_1 and b_2 (and zero for the others), the result is a force of about 1 N. Using a space object mass of about 340 kg, the acceleration is approximately 0.003 m/s^2 , causing the space objects to move apart in 20–30 s. So, an operational system will have to compensate for this tangential repulsion.

Converting Eq. (39) to Cartesian components, the torque density can be written

$$\begin{aligned}\vec{\tau} \times (\vec{J} \times \vec{B}) &= \sum_{n=1}^{\infty} b_n \sigma a^2 \omega B_r \left\{ \left[-\sin^2 \phi P_n^0(\cos \theta) + \frac{\cos 2\phi \cot \theta P_n^1(\cos \theta)}{n(n+1)} \right] \hat{x} \right. \\ &\quad \left. + \cos \phi \sin \phi \left[P_n^0(\cos \theta) + \frac{2\cot \theta P_n^1(\cos \theta)}{n(n+1)} \right] \hat{y} - \frac{\cos \phi P_n^1(\cos \theta)}{n(n+1)} \hat{z} \right\}. \quad (42)\end{aligned}$$

From Eq. (19) the total torque is found by integrating Eq. (42) over the volume of the material making up the hollow sphere. Integrating with respect to ϕ causes all of the terms in curly braces except one to go to zero and that one term contains a single zeroth-order Legendre polynomial

$$\vec{\tau} = -\pi \sigma a^4 \omega h \sum_{n=1}^{\infty} b_n \int_0^{\pi} B_r P_n^0(\cos \theta) \sin \theta d\theta \hat{x}. \quad (43)$$

After using the expression for B_r in Eq. (29) and the orthogonality condition (B11) the θ -integration can be performed, leaving a surprisingly simple result

$$\vec{\tau} = -2\pi \sigma a^4 \omega h \sum_{n=1}^{\infty} \frac{b_n^2}{2n+1} \hat{x}. \quad (44)$$

In addition, Eq. (29) can also be used to express the torque as the integral of the radial magnetic field component squared

$$\vec{\tau} = -\pi \sigma a^4 \omega h \int_0^{\pi} B_r^2 \sin \theta d\theta \hat{x}, \quad (45)$$

an intriguing result.

Meanwhile, the decay time [see Eqs. (20)–(22)] becomes

$$\alpha = \frac{4\rho_m}{3\sigma \sum_{n=1}^{\infty} b_n^2 / (2n+1)}. \quad (46)$$

When the applied field is uniform, $b_1 = B$ and all other components are zero so this equation reduces to Eq. (22), as expected. Equation (46) will determine if we can de-spin a space object and a cursory examination of it bodes well for this concept. Assuming an aluminum space object and a 1 mT field component, the time period given by Eq. (46) is less than an hour, which implies the concept is feasible. We plan on studying Eq. (46) with the intent of minimizing the

decay time under a set of space object limitations such as approach distance, available power, and magnet mass allowance. However, this is best left for a more specialized paper. Instead, we will describe a pair of experiments that validate Eqs. (22) and (46), the decay time predictions for uniform and non-uniform applied fields, respectively.

VII. EXPERIMENTAL RESULTS

The torque predictions made above can be tested by hanging a hollow conducting sphere by a thin thread and measuring the decay in the amplitude of its torsional oscillations first without and then with an applied magnetic field. In the lossless case, the torque equation is given by

$$\tau = I\dot{\omega} = -\kappa\theta, \quad (47)$$

where $\dot{\omega}$ represents the time derivative of the angular velocity, κ is the torsion constant of the thread, and θ is the rotation angle of the sphere measured relative to its rest position. In the present case, there are two loss terms, one due to frictional losses (e.g., air resistance) and one to magnetic drag, both of which are proportional to the angular velocity of the sphere. Adding these to Eq. (47) and taking the derivative with respect to time yield a second-order differential equation for the angular velocity

$$\ddot{\omega} = -\left(\frac{1}{\alpha} + \frac{1}{\gamma}\right)\dot{\omega} - \frac{\kappa}{I}\omega, \quad (48)$$

where α and γ correspond to the magnetic and frictional damping, respectively. The moment of inertia has been absorbed into these damping terms, and they are defined as reciprocals so that they will have units of time. By doing this, the magnetic decay time α shown here is the same decay time as appears in Eqs. (22) and (46).

Solving Eq. (48) in the underdamped case, where the frictional and magnetic losses are small, shows that the sphere should oscillate with a period given by $2\pi\sqrt{I/k}$ and with an amplitude that decays exponentially as

$$\exp\left[-\frac{t}{2}\left(\frac{1}{\alpha} + \frac{1}{\gamma}\right)\right] = \exp\left(-\frac{t}{\delta}\right), \quad (49)$$

where δ is the total decay time. So by measuring the decay in the oscillation of hanging sphere without a magnetic field, the frictional damping term γ can be found. Then, by applying the magnetic field, the total decay time δ can be found, allowing the magnetic decay time α to be found from the relationship

$$\frac{1}{\alpha} = \frac{2}{\delta} - \frac{1}{\gamma}. \quad (50)$$

We purchased a Helmholtz coil, as shown in Fig. 7, with 150 turns per coil and a 150 mm coil radius and coil spacing. Flowing 3 A of current through the coils generates a magnetic field of about 0.0023 T as measured by a Gauss-meter. We hung a 5-in. diameter, 0.132-in. wall thickness, hollow aluminum sphere (alloy 3003) in the center of the Helmholtz coil using a fine steel wire with a length of about 0.5 m.

In order to measure the relative rotation angle of the sphere, a small flat reflector was attached to the wire near the support point. As the sphere oscillates, with a starting

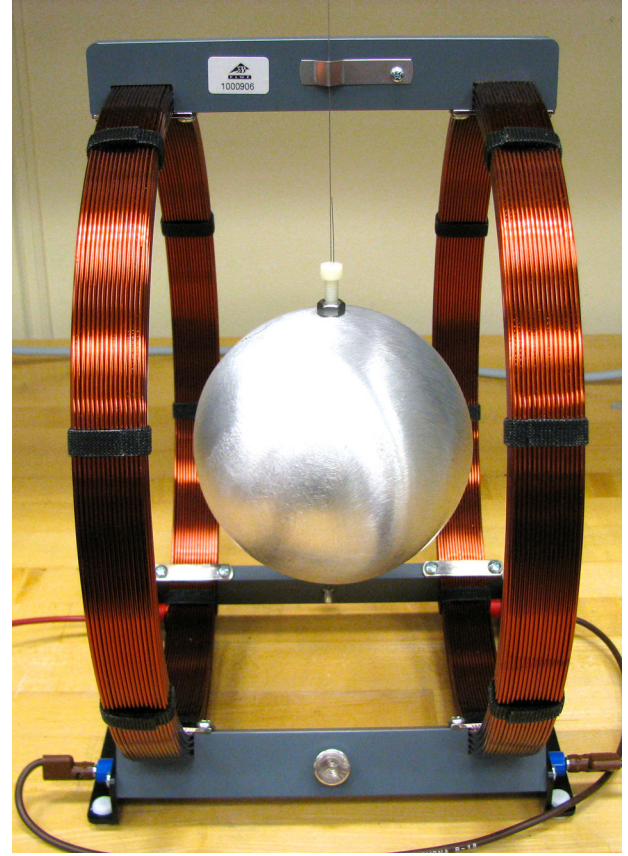


Fig. 7. (Color online) A hollow aluminum sphere hanging by a thin steel wire in a Helmholtz coil.

amplitude of 10–20 radians, this reflector rotates through a proportionally smaller angle, such that it always stays in view of a laser distance monitor. The measured distance to the reflector is sent to a computer and later converted to an angle. Because we are only concerned with the decay times, this relative angle versus time is sufficient to obtain the magnetic decay time.

Figure 8 shows the relative oscillation amplitude of the sphere in the Helmholtz coil with and without the magnetic field present. Clearly, the magnetic field provides a significant damping effect. From Eq. (22), the magnetic decay time should be $4\rho_m/(\sigma B^2)$. The density of aluminum is 2700 kg/m^3 ,

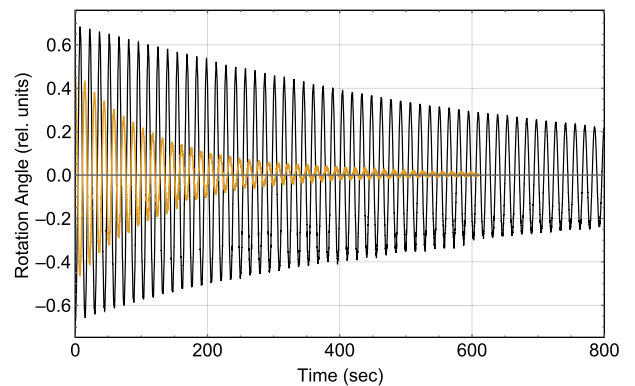


Fig. 8. (Color online) Plots of the rotation angle of the hollow sphere (relative units) shown in Fig. 7 versus time with the Helmholtz coil turned off (black) and on (gray, tan).

and the conductivity of 3003 aluminum ranges from 2.38×10^7 to 2.94×10^7 S/m, so the decay time should be between 69 and 86 s. We used MATHEMATICA to fit the data in Fig. 8 to a decaying exponential and obtained 725 s without the magnetic field and 125 s with it. So the frictional damping term is $\gamma = 363$ s, and the total decay time is $\delta = 125$ s. Using Eq. (50), the magnetic decay time is $\alpha = 75.5$ s, which is in good agreement with prediction. If we assume Eq. (22) is correct, then we can deduce that the conductivity of the sphere is 2.7×10^7 S/m.

In our next experiment, we placed a single, smaller coil 150 mm from the center of a larger, 4-in. radius, hanging sphere as shown in Fig. 9. This coil has 320 turns of wire with a radius of about 0.07 m and was driven with a current of 2 A. We measured the magnetic field from this coil and compared it with the standard form for the magnetic field from a thin coil.²² The agreement was sufficiently close that we decided to use this analytical expression to calculate the Legendre polynomial decomposition coefficients (b_n), using MATHEMATICA to numerically solve Eq. (30). Writing these in units of mT, the first six values are 0.514, 0.89, 0.963, 0.803, 0.54, and 0.29, with the higher-order values dropping in size after that. Placing these into Eq. (46) yields a predicted decay time of 275 s.

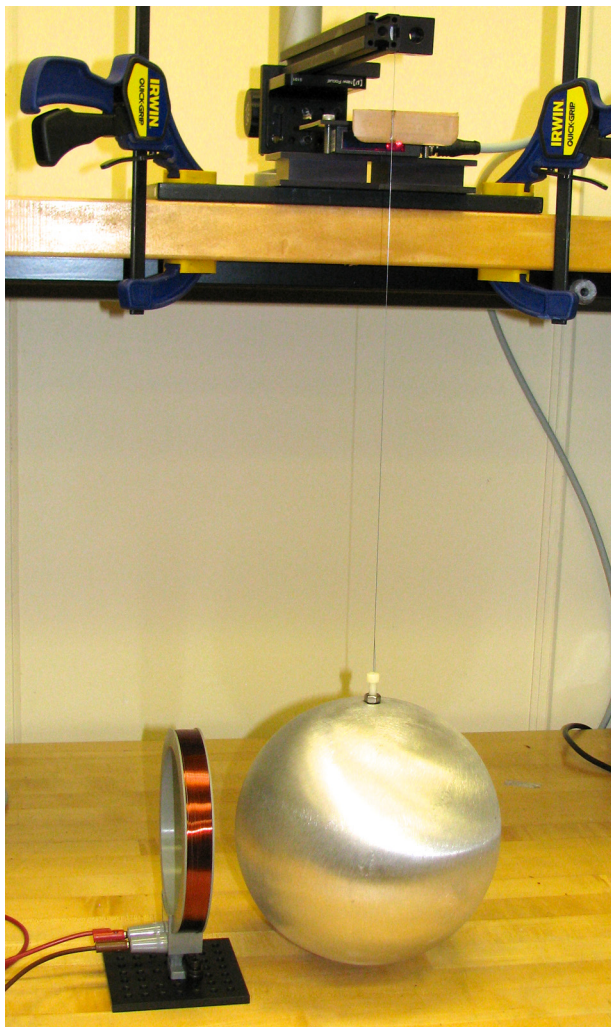


Fig. 9. (Color online) A 4-in. radius hollow aluminum sphere hanging from a thin steel wire undergoes torsional oscillations in a non-uniform magnetic field created by a single coil.

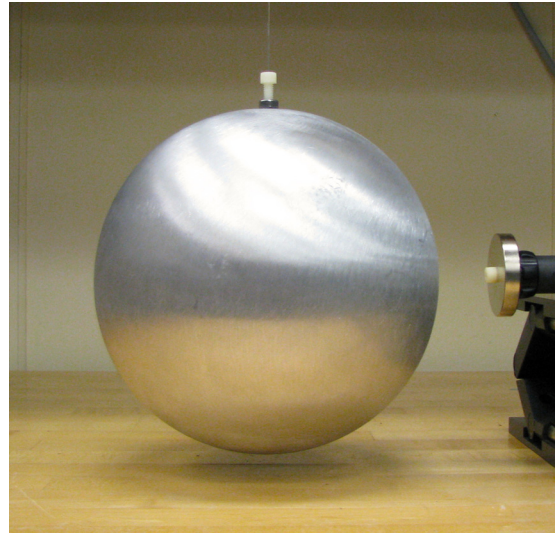


Fig. 10. (Color online) A 4-in. radius hollow aluminum sphere undergoes torsional oscillations in a non-uniform magnetic field created by a small rare-earth magnet.

With the magnetic field turned on, the sphere's rotation damped out with a time constant of 458 s, and without the magnetic field the decay time was 2282 s ($\gamma = 1141$ s). This much longer decay time from the first experiment is due to the use of a significantly larger, more massive, sphere. Combining the two decay times yields a magnetic decay time of 286 s, which is within 4% of the theory.

In our last experiment, we placed a rare-earth magnet 15 cm to the side of the large 4-in. radius hollow sphere, as shown in Fig. 10. The magnet is 2 in. of diameter and 3/8 in. thick. Based on magnetic field measurements, we modeled it as an air-core coil of the same size with a total current of 9000 A. Performing a decomposition into Legendre polynomials, we obtained the first 14 values (in mT) of 1.036,

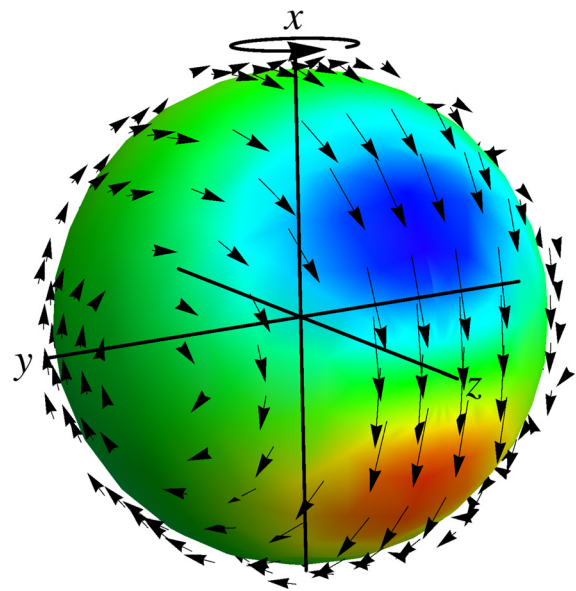


Fig. 11. (Color online) The predicted charge and current density created by the interaction of the 4-in. radius rotating aluminum sphere with a 2-in. diameter rare-earth magnet located 15 cm to one side along the z-axis. The positive charge (red) lies in the $-x, +z$ quadrant, while the negative (blue) charge is in the $+x, +z$ quadrant.

2.034, 2.64, 2.84, 2.73, 2.43, 2.04, 1.64, 1.27, 0.95, 0.69, 0.49, 0.34, and 0.23; after that the values decay rapidly. Because the size of the magnet is relatively small, it is reasonable that the decomposition extends to higher-order polynomials. Substituting these into Eq. (46) predicts a decay time of 27.9 s.

When we ran the experiment with the rare-earth magnet, we measured a decay time of 54.1 s. Removing the frictional decay contribution ($\gamma = 1141$ s) yields a magnetically induced decay time of 27.7 s, remarkably close to the prediction (less than 1% difference).

Using Eqs. (36) and (38), the charge and current densities created by the interaction of the sphere's rotation and the rare-earth magnet can be found. Using MATHEMATICA and working to 25 orders in the Legendre polynomials yields the result shown in Fig. 11 (compare to Fig. 6). The magnetic field is applied along the z -axis, causing a charge displacement along the x -axis direction. The current flows between these two charge densities and then loops around the rest of the sphere.

VIII. CONCLUSIONS

We have demonstrated the feasibility of de-spinning a defunct satellite or a piece of space debris with an applied magnetic field by redeveloping an analysis published by Hertz¹¹ in 1880. The development is instructive for advanced students of electro-magnetism, because it utilizes multiple concepts applied to a very modern problem, yet is placed into a historical setting. Experiments were performed to validate the theory using equipment that could be set up in a physics laboratory allowing students to examine the forces, torques, and magnetic field interactions that occur when a sphere is allowed to slowly spin in an applied magnetic field. Finally, the results show promise for using a magnetic field to de-spin an orbiting space object. Further work in this area is warranted based on the results demonstrated here. We plan to extend the previous work published by one of the authors

to include the effects of time varying magnetic fields on satellites.^{23,24}

ACKNOWLEDGMENTS

The authors would like to acknowledge the many insightful comments provided by the reviewers that greatly improved the quality of this paper.

APPENDIX A: A SOLUTION TO POISSON'S EQUATION

This Appendix provides the solution for the potential $\Phi(r, \theta, \phi)$, given a thin-walled conducting spherical shell of (mean) radius a and thickness h with a radially independent charge distribution $\rho_t(\theta, \phi)$.¹⁵ The potential inside and outside the shell are described by Laplace's equation while Poisson's equation is needed within the shell due to the charge distribution. Thus, we need to solve

$$\nabla^2 \Phi(r, \theta, \phi) = \begin{cases} 0, & r < a - \frac{h}{2} \\ -\rho_t(\theta, \phi)/\epsilon_0, & a - \frac{h}{2} \leq r \leq a + \frac{h}{2} \\ 0, & r > a + \frac{h}{2}. \end{cases} \quad (\text{A1})$$

If the charge distribution can be described by a spherical harmonic

$$\rho_t(\theta, \phi) = \epsilon_0 b P_n^m(\cos \theta) \cos(m\phi + \phi_0), \quad (\text{A2})$$

where b and ϕ_0 are arbitrary constants, then the bounded and continuous solution is

$$\Phi(r, \theta, \phi) = \begin{cases} \frac{ba^2 r^n}{n(n+1)(a-h/2)^n} P_n^m(\cos \theta) \cos(m\phi + \phi_0), & r < a - \frac{h}{2} \\ \frac{ba^2}{n(n+1)} P_n^m(\cos \theta) \cos(m\phi + \phi_0), & a - \frac{h}{2} \leq r \leq a + \frac{h}{2} \\ \frac{ba^2(a+h/2)^{n+1}}{n(n+1)r^{n+1}} P_n^m(\cos \theta) \cos(m\phi + \phi_0), & r > a + \frac{h}{2}. \end{cases} \quad (\text{A3})$$

APPENDIX B: LEGENDRE POLYNOMIAL RELATIONSHIPS

The following Legendre polynomial relationships²⁵ were used to derive some of the results given in this paper. Although these relationships can be found in many places, we felt it would be useful to include them here for completeness

$$P_2^0(\cos \theta) = \cos^2 \theta - \frac{1}{2} \sin^2 \theta = \frac{1}{4}(1 + 3 \cos 2\theta), \quad (\text{B1})$$

$$P_2^1(\cos \theta) = -3 \cos \theta \sin \theta, \quad (\text{B2})$$

$$\frac{\partial}{\partial \theta} [\sin^2 \theta P_n^0(\cos \theta)] = \sin \theta [(n+1)P_{n+1}^0(\cos \theta) - (n-1)\cos \theta P_n^0(\cos \theta)], \quad (\text{B3})$$

$$\cos \theta P_n^0(\cos \theta) = \frac{1}{2n+1} [(n+1)P_{n+1}^0(\cos \theta) + nP_{n-1}^0(\cos \theta)], \quad (\text{B4})$$

$$\frac{\partial}{\partial \theta} [P_{n+1}^0(\cos \theta) - P_{n-1}^0(\cos \theta)] = -(2n+1) \sin \theta P_n^0(\cos \theta), \quad (\text{B5})$$

$$\sin \theta P_n^0(\cos \theta) = \frac{1}{2n+1} [P_{n-1}^1(\cos \theta) - P_{n+1}^1(\cos \theta)], \quad (\text{B6})$$

$$\cos \theta \frac{\partial P_n^0(\cos \theta)}{\partial \theta} = -\frac{1}{2n+1} [(n+1)P_{n-1}^1(\cos \theta) + nP_{n+1}^1(\cos \theta)], \quad (\text{B7})$$

$$\cos \theta P_n^1(\cos \theta) = -\frac{1}{2n+1} [(n+1)P_{n-1}^1(\cos \theta) + nP_{n+1}^1(\cos \theta)], \quad (\text{B8})$$

$$-\frac{1}{n(n+1)} \frac{\partial [\cos \theta P_n^1(\cos \theta)]}{\partial \theta} - \cos \theta P_n^0(\cos \theta) = -\frac{1}{2} \left[P_{n-1}^0(\cos \theta) - \frac{P_{n-1}^2(\cos \theta)}{n(n+1)} \right], \quad (\text{B9})$$

$$-\frac{\cos \theta}{n(n+1) \sin \theta} P_n^1(\cos \theta) + P_n^0(\cos \theta) = \frac{1}{2} \left[P_n^0(\cos \theta) - \frac{P_n^2(\cos \theta)}{n(n+1)} \right], \quad (\text{B10})$$

$$\int_0^\pi P_n^0(\cos \theta) P_m^0(\cos \theta) \sin \theta d\theta = \frac{2}{2n+1} \delta_{nm}. \quad (\text{B11})$$

^{a)}Electronic mail: Robert.C.Youngquist@nasa.gov

^{b)}Author to whom correspondence should be addressed. Electronic mail: Mark.A.Nurge@nasa.gov

^{c)}Electronic mail: Stanley.O.Starr@nasa.gov

^{d)}Electronic mail: frederick.levy@us.af.mil

^{e)}Electronic mail: mp336@cornell.edu

¹J. P. Vinti, "Theory of the spin of a conducting space object in the magnetic field of the Earth," Ball. Res. Lab., Report No. 1020, 1957, available at <<http://www.dtic.mil>> with a DTIC issued certificate to access controlled documents.

²H. B. Rosenstock, "The effect of the Earth's magnetic field on the spin of the satellite," *Astronautica acta* **101**, 215–221 (1957).

³N. Sanduleak, "A generalized approach to the magnetic damping of the spin of a metallic Earth satellite," Army Ballistic Missile Agency, Redstone Arsenal, Report No. DG-TM-151–158, 1958, available at <<http://www.dtic.mil>> with a DTIC issued certificate to access controlled documents.

⁴G. L. Smith, "A theoretical study of the torques induced by a magnetic field on rotating cylinders and spinning thin-wall cones, cone frustums, and general body of revolution," NASA Tech. Rep. R-129, Langley Research Center, 1962, <<http://ntrs.nasa.gov/archive/nasa/casi.ntrs.nasa.gov/19630002720.pdf>>.

⁵J. F. Ormsby, "Eddy current torques and motion decay on rotating shells," No. MTR-224, MITRE Corp., Bedford, MA, 1967, <<http://www.dtic.mil/docs/citations/AD0664338>>.

⁶R. H. Wilson, "Magnetic effects on space vehicles and other celestial bodies," *Irish Astron. J.* **13**, 1–13 (1977); available at <http://adsabs.harvard.edu/full/1977IrAJ...13....1W>.

⁷R. H. Wilson, "Magnetic damping of rotation of satellite 1958β2," *Science* **130**(3378), 791–793 (1959).

⁸L. LaPaz and R. H. Wilson, "Magnetic damping of rotation of the Vanguard I satellite," *Science* **131**(3397), 355–357 (1960).

⁹N. Praly *et al.*, "Study on the eddy current damping of the spin dynamics of space debris from the Ariane launcher upper stages," *Acta Astronaut.* **76**, 145–153 (2012).

¹⁰C. Babbage and J. F. W. Herschel, "Account of the repetition of M. Arago's experiments on the magnetism manifested by various substances during the act of rotation," *Phil. Trans. R. Soc. London* **115**, 467–496 (1825).

¹¹H. Hertz, "On the induction in rotating spheres, 1880," *Miscellaneous Papers* (Macmillan and Co. Ltd, London, 1896), see Sec. 2, pp. 35–126.

¹²T. Bennett *et al.*, "Prospects and challenges of touchless space debris despinning using electrostatics," *Adv. Space Res.* **56**(3), 557–568 (2015).

¹³N. O. Gómez and S. J. I. Walker, "Eddy currents applied to de-tumbling of space debris: Analysis and validation of approximate proposed methods," *Acta Astronaut.* **114**, 34–53 (2015).

¹⁴C. J. Wetterer *et al.*, "Refining space object radiation pressure modeling with bidirectional reflectance distribution functions," *J. Guid. Cont. Dyn.* **37**(1), 185–196 (2013).

¹⁵J. D. Jackson, *Classical Electrodynamics*, 3rd ed. (John Wiley & Sons, Inc., New York, NY, 1999), p. 110.

¹⁶J. Schwinger *et al.*, *Classical Electrodynamics* (Westview Press, Boulder, CO, 1998).

¹⁷P. Lorrain and D. Corson, *Electromagnetic Fields and Waves*, 2nd ed. (W. H. Freeman & Co. Ltd., New York, NY, 1970), Appendix C, pp. 657–664.

¹⁸D. J. Griffiths, *Introduction to Electrodynamics*, 3rd ed. (Prentice Hall, Upper Saddle River, NJ, 1999), pp. 236–237, 298–299, and inside back cover.

¹⁹R. P. Halverson and H. Cohen, "Torque on a spinning hollow sphere in a uniform magnetic field," *IEEE Trans. Aerosp. Navig. Electron.* **2**, ANE-11 (1964).

²⁰P. Lorrain, "Electrostatic charges in $\mathbf{v} \times \mathbf{B}$ fields: The Faraday disk and the rotating sphere," *Euro. J. Phys.* **11**(2), 94–98 (1990).

²¹The terminology, "advection current" isn't prominent in literature, but the adjective "advection" seems fitting to describe this current. There is an apparent current due to the motion of the charges as they are carried around by the turning of the sphere, similar to the way a floating leaf is carried along by a river. There is no Ohmic loss, yet the charges are in motion.

²²J. C. Simpson *et al.*, "Simple analytic expressions for the magnetic field of a circular current loop," NASA Tech. Mem., NASA/TM-2013-217919, 2013, <http://ntrs.nasa.gov/archive/nasa/casi.ntrs.nasa.gov/20140002333.pdf>.

²³B. Reinhardt and M. A. Peck, "Eddy-Current Space Tug," AIAA Space 2011 Conference and Exposition, September 27–29, 2011.

²⁴B. Z. Reinhardt, B. Hency, and M. Peck, "Characterization of eddy currents for space actuation," AIAA/AAS Astrodynamics Specialist Conference, August 13–16, 2012.

²⁵Wikipedia contributors, Associated Legendre polynomials, Wikipedia, The Free Encyclopedia, May 18, 2015, 08:57 UTC, available at <https://en.wikipedia.org/w/index.php?title=Associated_Legendre_polynomials&oldid=662909365> (accessed September 2, 2015).